IEEE Access
Multidisciplinary | Rapid Review | Open Access Journal

Received July 20, 2018, accepted September 2, 2018, date of publication November 9, 2018, date of current version November 30, 2018.

Digital Object Identifier 10.1109/ACCESS.2018.2869461

Non-Local Means Image Denoising Using Shapiro-Wilk Similarity Measure

W. YAMANAPPA[1], P. V. SUDEEP[2], M. K. SABU[3], AND JENY RAJAN[1]
[1]Department of Computer Science and Engineering, National Institute of Technology Karnataka, Mangalore 575025, India
[2]Department of Electronics and Communication Engineering, National Institute of Technology Calicut, Kozhikode 673601, India
[3]Department of Computer Applications, Cochin University of Science and Technology, Kochi 682022, India

Corresponding author: W. Yamanappa (yamanu.sjce06@gmail.com)

ABSTRACT Most of the real-time image acquisitions produce noisy measurements of the unknown true images. Image denoising is the post-acquisition technique to improve the signal-to-noise ratio of the acquired images. Denoising is an essential pre-processing step for different image processing applications such as image segmentation, feature extraction, registration, and other quantitative measurements. Among different denoising methods proposed in the literature, the non-local means method is a preferred choice for images corrupted with an additive Gaussian noise. A conventional non-local means filter (CNLM) suppresses noise in a given image with minimum loss of structural information. In this paper, we propose modifications to the CNLM algorithm where the samples are selected statistically using Shapiro–Wilk test. The experiments on standard test images demonstrate the effectiveness of the proposed method.

INDEX TERMS Denoising, Gaussian, non-local means, noise, Shapiro-Wilk test.

I. INTRODUCTION

Noise is a random variation of image intensity values that makes the visual analysis and other post-processing operations difficult. The presence of noise is unavoidable in images and its contamination depends on how the image is created. Denoising suppresses the adverse impact of noise in the acquired images and is an important pre-processing step to increase the SNR of the image which is important for image segmentation, feature extraction, texture analysis etc. [1]. The aim of image denoising is to reduce the noise while preserving the edges and other fine details in the image as much as possible.

Different approaches proposed in the literature to enhance image quality by reducing the noise can broadly be classified into two categories; spatial domain methods [2]–[4] and transform domain methods [5]–[7]. Depending on the way of finding the candidate pixels, spatial domain methods are further classified into local and non-local filtering. Mean filter, Median filter, Gaussian filter [2], Least-Mean-Square Adaptive Filters [3], anisotropic filtering [4], bilateral filter [8],steering kernel regression filter [9] etc. are examples for spatial filters based on local statistics. The filters that uses transformation such as wavelet transform [5], contourlet transform [6], curvelet transform [6], principal component analysis [7], singular value decomposition [10] or discrete cosine transform [11] are examples of transform domain filters. Most of the aforementioned methods blur fine details in the images while denoising.

Buades *et al.* [30], [31] proposed a non-local weighted averaging method based on patch similarity to estimate the true underlying intensity of pixels from the given noisy image. The estimates are nonlocal because, the pixels that are not in the immediate neighborhood of the pixel of interest are also considered for weighted averaging. The performance of conventional NLM (CNLM) algorithm depends on the similarity measure used, the decay parameter and search and similarity window size. Several authors have proposed different NLM frameworks to optimize any of these parameters to enhance the denoising performance or reducing the computation time. Such a few NLM variants are listed in Table1. In this paper we improved the denoising performance of CNLM using Shapiro-Wilk test as similarity measure instead of Euclidean distance (used in CNLM).

The rest of the paper is organized as follows: the relevant background on the noise model, conventional NLM filter and the Shapiro-Wilk test are discussed in Section 2. Section 3 explains the proposed approach. Experimental results are reported in Section 4 and the paper is concluded in Section 5.

TABLE 1. Different NLM based filters for image denoising.

Sl.No.	Year	Authors	Remarks
1	2015	Cai, Bin *et al.* [13]	Similarity measure based on local binary pattern (LBP) operator
2	2015	R.Verma *et al.* [14]	added adaptive isotropic search window map using gray level difference image.
3	2015	Chenglin Zuo [15]	employed local frequency driscriptors to measure the similarity
4	2014	Bhujle *et al.* [16]	Dictionary based NLM to reduce computational cost
5	2013	Y. Zhan [17]	pixel-wise decay parameter adaption using golden section search method
6	2012	Chaudhury *et al.* [18]	replaced mean by Eucledian median at large noise levels
7	2012	R. Yan *et al.* [19]	integrated Gaussian blur, clustering, and rotationally invariant block matching
8	2012	C. A. Deledalle *et al.* [20]	fast implementation of NL-Means based on FFT calculations
9	2011	G. Sven [21]	Combined the structure tensor with rotationally invariant block matching
10	2011	W. L. Zeng [22]	adaptive NLM by choosing the patch size according to region characteristics.
11	2010	K. Zheng *et al.* [23]	adaptive NLM based on the region via pixel region growing and merging.
12	2010	V. Duval *et al.* [24]	introduced automatic parameter tuning in spatially adaptive NLM
13	2010	Vignesh *et al.* [25]	deduced computation by probabilistic early termination
14	2009	Zexuan Ji *et al.* [26]	Combined Zernike moments to get similarity
15	2009	Yifei Lou *et al.* [27]	used SIFT like descriptors to obtain similar patches
16	2008	Zimmer *et al.* [28]	used similarity measure invariant under rotations and mirroring and Hu moment
17	2008	Liu *et al.* [29]	integrated laplacian pyramid and NLM
18	2007	Brox *et al.* [30]	an iterated NLM with a sorting criterion

II. THEORY

A. THE AWGN MODEL

The noisy image V is a two dimensional array of pixels and can be modeled mathematically as

$$V = U + \eta \tag{1}$$

where U represents the underlying clean image and η is the noise component independent to U. This statistical uncertainty η is assumed to be an additive zero mean white Gaussian noise (AWGN) with standard deviation σ. Although we consider the case of AWGN in this paper, the proposed approah can be extended to other noise models like Rician by incorporating the noise properties and extending the NL-Means as in [32]. Most of the denoising algorithms require the estimate of noise level for better denoising performance. In this paper, we estimated the noise standard deviation $\hat{\sigma}$ from the noisy image as explained in [33],

$$\hat{\sigma^2} = \quad \text{mode}\,\{\sigma_{N_i}^2\} \tag{2}$$

where $\sigma_{N_i}^2$ represents the local variance estimated from the neighborhood N_i around each pixel i. We used the neighborhood window of size 7×7 to compute the local variance.

B. CONVENTIONAL NON-LOCAL MEANS FILTER (NLM)

The non-local means filter [31] is widely used due to its simplicity and efficiency in denoising images. It makes use of the self-similarity of pixels in the image and well suited to AWGN noise model. The NLM algorithm performs a weighted sum approach in which the algorithm updates a pixel's value with the weighted sum of pixels in the search area based on the similarity of neighborhoods computed using Euclidean distance. Consider the observed image $V = \{v(y) | y \in \mathbb{R}^2\}$, where $v(y)$ corresponds to the noisy image value at pixel location y. Now the true underlying value of the pixel at location r is computed as [31], [32], [34]:

$$NL(v(r)) = \sum_{\forall s \in \Omega} w(r,s)\, v(s) \tag{3}$$

where $v(s)$ represent the non-local pixels in the search window Ω and w is the normalized weight which is computed as:

$$w(r,s) = \frac{1}{Z(r)} e^{-\frac{d(r,s)}{h^2}} \tag{4}$$

where h is the smoothing parameter. In most implementations of NLM, the parameter h is taken as the noise standard deviation. $Z(r)$ is the normalizing constant computed as,

$$Z(r) = \sum_{\forall s \in \Omega} e^{-\frac{d(r,s)}{h^2}}. \tag{5}$$

The distanc d in Eq. 4 is defined as,

$$d(r,s) = G_\sigma \|N_r - N_s\|_{l_2}^2 \tag{6}$$

where G_σ is a Gaussian kernel with mean zero and standard deviation σ. The blocks N_r and N_s denote the neighborhood pixels around r^{th} and s^{th} pixel of V respectively. The self similarity will be maximum when $r = s$ and produces an over-weighting effect. To avoid it, we calculated $w(r,r)$ as,

$$w(r,r) = \max(w(r,s) \forall s \neq r). \tag{7}$$

C. SHAPIRO-WILK PARAMETRIC HYPOTHESIS TEST OF COMPOSITE NORMALITY (SW TEST)

There are different goodness-of-fit tests such as Kolmogorov-Smirnov (KS test) [35], Anderson-Darling test (AD test) [35], T-test, χ^2 test, Jarque-Bera test (JB test) [36], Shapiro-Wilk test (SW test) [37] etc. for checking normality and to make inferences about data. Among them, SW test based on W statistic is one of the mostly known and applied test to check

Algorithm 1 SW-NLM Filter

Input: $V \Leftarrow$ Noisy image
  $\hat{\sigma} \Leftarrow$ Noise standard deviation computed using Eq. 2.
for each pixel $v(x)$ of V **do**
  Initialize $W_{max} = 0$,$Average = 0$,$Sumweights = 0$.
  Select a $T \times T$ *SearchWindow* around the pixel
  $N_x \Leftarrow$ *Similaritywindow* of size $t \times t$ around the pixel
  $N_y \Leftarrow$ Non local neighbourhood windows in the *SearchWindow* other than N_x
  for each N_y **do**
    Compute the difference $D = (N_x - N_y)$ and find N_D using Eq. 12.
    Apply Shapiro-Wilk Test on N_D and find both statistic value W and hypothesis H.
    Compute the statistical parameters of N_D: Mean μ_{N_D} and standard deviation σ_{N_D}
    Apply Eq. 13 to find the standard error (SE) of N_D
    C=0
    if $(SE > \mu_{N_D} > -SE)$ and $(1 + SE > \sigma_{N_D} > 1 - SE)$ and hypothesis H_0 **then**
      C=1
    end if
    compute weight $W' = C \times W$
    if $(W' > W_{max})$ **then**
      $W_{max} = W'$
    end if
    $Sumweights = Sumweights + W'$
    $Average = Average + W' \times v(y)$
  end for
  $Average = Average + W_{max} \times v(x)$
  $Sumweights = Sumweights + W_{max}$
  if $(Sumweights > 0)$ **then**
    $\hat{u}(x) = Average/Sumweights$
  else
    $\hat{u}(x) = v(x)$
  end if
end for
Output: $\hat{U} \Leftarrow$ Denoised image

normality of a given distribution when sample size is small. The Shapiro-Wilk W statistic is defined as [37]:

$$W = \frac{\left(\sum_{i=1}^{n} a_i X_{(i)}\right)^2}{\left(\sum_{i=1}^{n} X_i - \bar{X}\right)^2} \tag{8}$$

where $X_{(1)} \leq X_{(2)} \leq \cdots \leq X_{(n)}$ are the ordered value of the samples $(X_1, X_2, \cdots, X_n)$, $\bar{X}$ is the sample mean and a_i are tabulated coefficients [37]. The small values for W statistics indicate non-normality and is always $0 < W \leq 1$. The SW test can be used for any n in the range $3 \leq n \leq 5000$ [38].

III. PROPOSED METHOD

It is a well known fact that the difference of two normal (Gaussian) distribution results in another normal distribution. That means, the distribution of difference of two normally distributed variates Θ and Ψ with mean and standard deviation $(\mu_\theta, \sigma_\theta)$ and (μ_ψ, σ_ψ) respectively is a normal distribution given by [39]:

$$P_{\Theta-\Psi}(u|\Theta, \Psi, \sigma_\theta, \sigma_\psi) = \int_{-\infty}^{\infty}\int_{-\infty}^{\infty} \frac{e^{-\theta^2/2\sigma_\theta^2}}{\sigma_\theta\sqrt{\pi}} \cdot \frac{e^{-\psi^2/2\sigma_\psi^2}}{\sigma_\psi\sqrt{\pi}} \delta((\theta - \psi) - u) d\theta d\psi \tag{9}$$

where $\delta(\theta)$ is a delta function. The mean and variance of the resultant normal distribution are :

$$\mu_{\Theta-\Psi} = \mu_\Theta - \mu_\Psi \tag{10}$$

and

$$\sigma^2_{\Theta-\Psi} = \sigma^2_\Theta + \sigma^2_\Psi \tag{11}$$

respectively. In this work we computed the similarity between two different patches by taking the difference between them. If those two patches are having the same underlying intensity then the difference patch D will be having a mean zero and standard deviation $\sqrt{2}\hat{\sigma}$; where $\hat{\sigma}$ is an estimate of the noise standard deviation obtained with Eq. 2. Since the noise level is same across the image, the standard deviation of any two patches with same underlying intensity will be $\sqrt{2}\hat{\sigma}$. We conducted this normality test using the Shapiro-Wilk (SW) test. Before performing the SW test we normalized D as follows to make it a standard normal distribution.

$$N_D = D/(\sqrt{2}\hat{\sigma}) \tag{12}$$

Our null-hypothesis of SW test is that the population follows a standard normal distribution.

Since our sample size is too small, we also considered the standard error in the implementation. The standard error calculation is a common practice to counteract for any incidental inaccuracies during the sample collection. If a large number of samples involved in the calculations of the mean, the standard error tends to be small. When the standard error is small, the data is said to be more representative of the true mean.

The standard error is defined as [40]

$$SE = \sigma_{N_D}/\sqrt{n} \tag{13}$$

where, n is the number of observations and σ_{N_D} is the standard deviation of N_D. Once the samples are selected the weighted average is computed (as in NLM) to estimate the true underlying intensity. However only the NL pixels that passed the test will be considered for averaging. The proposed non-local means denoising methodology with Shapiro-Wilk statistic similarity is explained in Algorithm 1.

In the following sections, we refer the new non-local means denoising methodology which relies on Shapiro-Wilk statistic similarity as SWNLM filter.

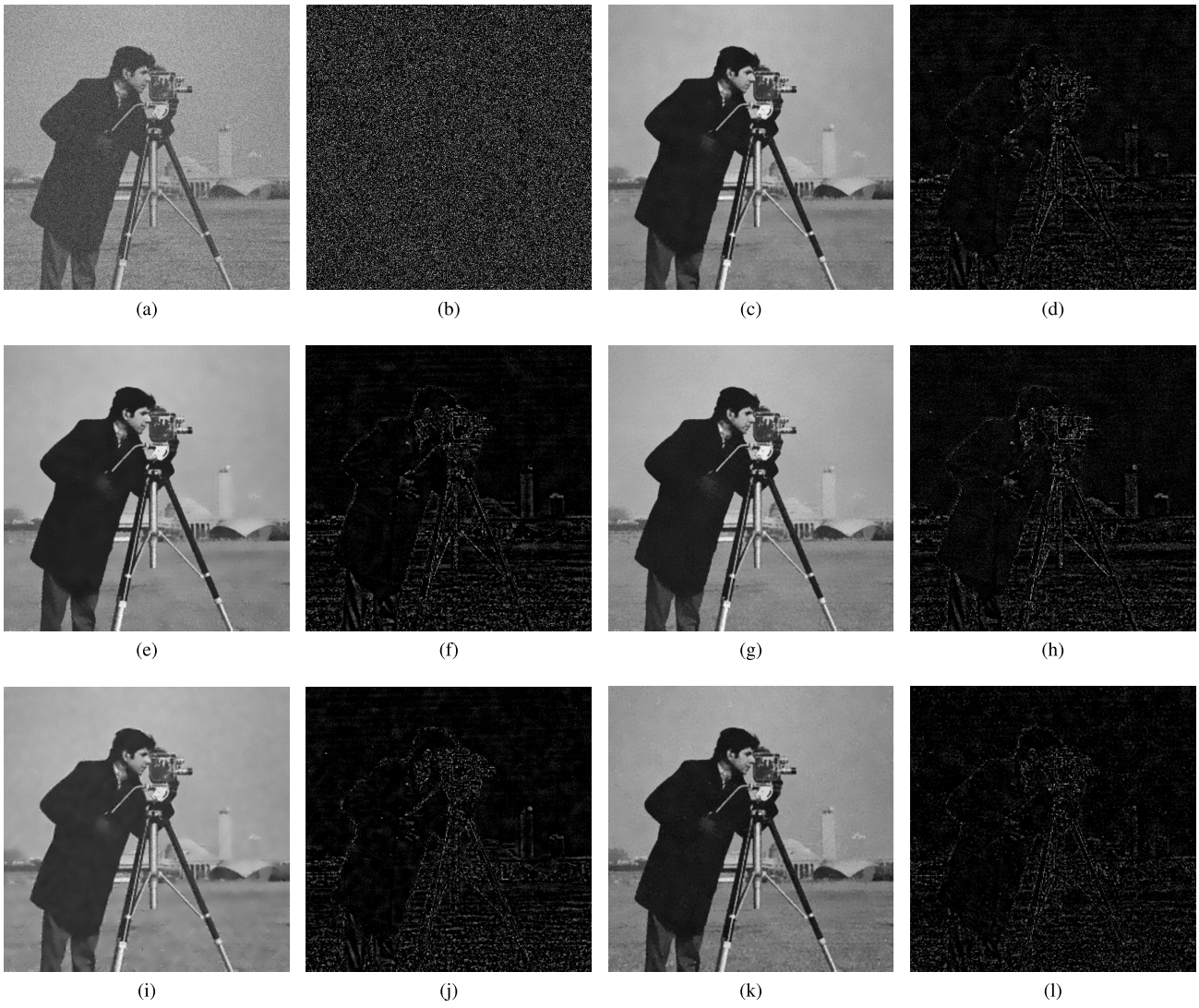

FIGURE 1. Denoising of Cameraman image with various methods (a) Noisy Cameraman image ($\sigma_g = 30$)(b) residual of image in (a) (c) Denoised image using CNLM filter (d) residual of image in (c) (e) Denoised image using PNLM filter (f) residual of image in (f) (g) Denoised image using JSNLM filter (h) residual of image in (g) (i) Denoised image using ANLM filter and (j) residual of image in (i) (k) Denoised image using SWNLM filter (l)residual of image in (k). (residuals in the range 0 – 70).

IV. EXPERIMENTS AND RESULTS

Experiments were conducted on different standard test images such as Cameraman image, Lena image, Boat image and Fingerprint image for validating and comparing the performance of the proposed method with other recently proposed methods. Results were evaluated both qualitatively and quantitatively. The proposed SWNLM method is compared with CNLM [30] and recently proposed NLM based methods such as NLM with probabilistic early termination (PNLM) [24], NLM with James Stein type center pixel weights (JSNLM) [42] and an adaptive isotropic search window based NLM (ANLM) [13] methods. For comparisons, all the above mentioned filters are executed with default settings and a search window of size of 21×21 and similarity window of size 3×3 respectively.

A. QUALITATIVE ANALYSIS

This section presents the results on Cameraman image and Fingerprint image for visual inspection. Fig. 1 and Fig. 2 shows the output of different denoising methods and their corresponding residual images in the intensity range [0,70] on Cameraman and Fingerprint images. It is clear from the figures (residual images) that the result by the proposed SWNLM filter surpasses the output by CNLM, PNLM, JSNLM and ANLM filters. In the fingerprint residual images, we can clearly observe that the image structural information is very less in the residual of the proposed method when compared to other images. Qualitatively, the proposed SWNLM filter performs well in preserving fine structures and has the superior noise removal capability over the other methods considered.

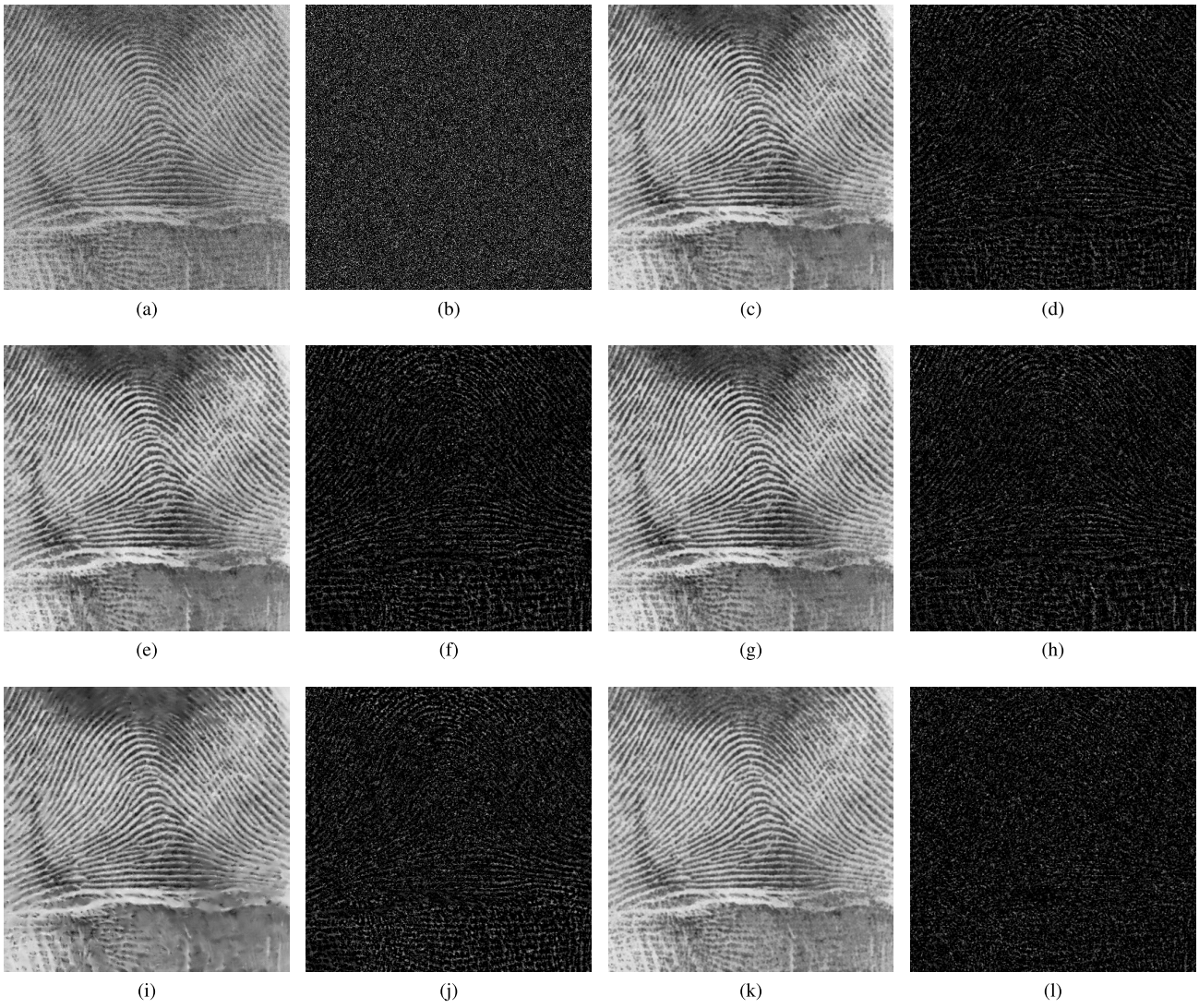

FIGURE 2. Denoising of Fingerprint image (Original image taken from [41])with various methods (a) Noisy Fingerprint image ($\sigma_g = 30$)(b) residual of image in (a) (c) Denoised image using CNLM filter (d) residual of image in (c) (e) Denoised image using PNLM filter (f) residual of image in (f) (g) Denoised image using JSNLM filter (h) residual of image in (g) (i) Denoised image using ANLM filter and (j) residual of image in (i)(k) Denoised image using SWNLM filter (l) residual of image in (k). (residuals in the range $0 - 70$).

TABLE 2. Comparison of experimental results on Cameraman image based on PSNR.

Method	PSNR								
	$\sigma = 5$	$\sigma = 10$	$\sigma = 15$	$\sigma = 20$	$\sigma = 25$	$\sigma = 30$	$\sigma = 35$	$\sigma = 40$	$\sigma = 45$
Noisy	34.1622	28.1229	24.6113	22.0941	20.1643	18.5972	17.2499	16.0922	15.0600
CNLM	39.4468	35.7828	33.3523	31.5539	30.1448	29.0230	28.0839	27.1164	26.2847
PNLM	39.7945	36.1507	33.7892	32.1499	30.9348	29.9777	29.0948	28.3825	27.6664
JSNLM	39.4200	35.6434	33.3696	31.6077	30.1753	29.0464	28.0453	27.1482	26.3503
ANLM	38.7424	35.1882	33.1297	31.7333	30.6572	29.6376	28.8696	28.0021	27.1332
SWNLM	39.7367	36.2879	34.3136	32.7809	31.5416	30.5451	29.6736	28.8220	28.1577

B. QUANTITATIVE ANALYSIS

We compared the performance of the proposed SWNLM filter and other aforementioned NLM filters on noisy images obtained by artificially corrupting standard images with AWGN noise. The noisy images are generated with different noise standard deviations ranges from 5 to 45. For comparison, we used the objective measures such as peak signal to noise ratio (PSNR) [43], mean structural similarity index matrix (SSIM) [44] and Bhattacharya coefficient (BC) [45].

PSNR is a popular quality measure that provide the overall quality of the image. On the other hand, mean SSIM gives

TABLE 3. Comparison of experimental results on Lena image based on PSNR.

Method	PSNR								
	$\sigma = 5$	$\sigma = 10$	$\sigma = 15$	$\sigma = 20$	$\sigma = 25$	$\sigma = 30$	$\sigma = 35$	$\sigma = 40$	$\sigma = 45$
Noisy	34.1426	28.1463	24.6235	22.1102	20.1594	18.5912	17.2515	16.1127	15.0756
CNLM	37.6832	34.5353	32.3740	30.7530	29.4703	28.3808	27.4253	26.5587	25.7784
PNLM	37.9224	34.6262	32.6371	31.1445	30.0201	29.0167	28.2186	27.5313	26.8994
JSNLM	37.7676	34.3182	32.1926	30.5656	29.2927	28.1762	27.2755	26.4158	25.5562
ANLM	37.6268	34.6208	32.8763	31.5433	30.3840	29.2630	28.2032	27.1817	26.1578
SWNLM	37.5562	34.5615	32.7389	31.4016	30.3237	29.4320	28.6009	27.8405	27.3156

TABLE 4. Comparison of experimental results on Boat image based on PSNR.

Method	PSNR								
	$\sigma = 5$	$\sigma = 10$	$\sigma = 15$	$\sigma = 20$	$\sigma = 25$	$\sigma = 30$	$\sigma = 35$	$\sigma = 40$	$\sigma = 45$
Noisy	34.1695	28.1256	24.5994	22.0998	20.1624	18.5947	17.2475	16.0944	15.0460
CNLM	36.9076	33.6619	31.4432	29.8511	28.5348	27.4993	26.5439	25.7450	24.9802
PNLM	36.4385	32.8886	30.8011	29.3429	28.2019	27.2046	26.3909	25.7282	25.0606
JSNLM	37.2592	33.3755	31.3004	29.6997	28.4588	27.3768	26.4269	25.5732	24.8981
ANLM	34.6778	32.5437	30.9142	29.6896	28.6514	27.7251	26.9114	26.0639	25.2494
SWNLM	37.1477	33.5330	31.6359	30.2925	29.2015	28.3380	27.5767	26.8917	26.1852

TABLE 5. Comparison of experimental results on Fingerprint image based on PSNR.

Method	PSNR								
	$\sigma = 5$	$\sigma = 10$	$\sigma = 15$	$\sigma = 20$	$\sigma = 25$	$\sigma = 30$	$\sigma = 35$	$\sigma = 40$	$\sigma = 45$
Noisy	34.1779	28.1634	24.5923	22.1264	20.1688	18.5815	17.2489	16.1083	15.0606
CNLM	34.3814	31.6035	29.5838	27.9500	26.5138	25.2985	24.1838	23.2209	22.3143
PNLM	35.1044	31.5882	29.6052	27.9245	26.5077	25.1844	24.0326	23.0895	22.1717
JSNLM	34.9613	31.6882	29.7858	28.1571	26.6970	25.4673	24.3680	23.3691	22.5408
ANLM	34.3149	29.8160	27.9281	26.6108	25.4676	24.4015	23.5110	22.6570	21.9013
SWNLM	34.5265	31.1574	29.6185	28.3351	27.1982	26.1893	25.2529	24.4494	23.7252

TABLE 6. Comparison of experimental results on Cameraman image based on mean SSIM.

Method	mean SSIM								
	$\sigma = 5$	$\sigma = 10$	$\sigma = 15$	$\sigma = 20$	$\sigma = 25$	$\sigma = 30$	$\sigma = 35$	$\sigma = 40$	$\sigma = 45$
Noisy	0.8134	0.5645	0.4086	0.3121	0.2486	0.2042	0.1721	0.1473	0.1277
CNLM	0.9642	0.9181	0.8605	0.7975	0.7366	0.6753	0.6145	0.5658	0.5166
PNLM	0.9641	0.9182	0.8620	0.7981	0.7349	0.6753	0.6186	0.5651	0.5156
JSNLM	0.9640	0.9208	0.8671	0.8070	0.7454	0.6869	0.6311	0.5786	0.5294
ANLM	0.9602	0.9281	0.8949	0.8620	0.8303	0.7924	0.7588	0.7113	0.6572
SWNLM	0.9687	0.9407	0.9106	0.8797	0.8449	0.8090	0.7755	0.7352	0.7076

TABLE 7. Comparison of experimental results on Lena image based on mean SSIM.

Method	mean SSIM								
	$\sigma = 5$	$\sigma = 10$	$\sigma = 15$	$\sigma = 20$	$\sigma = 25$	$\sigma = 30$	$\sigma = 35$	$\sigma = 40$	$\sigma = 45$
Noisy	0.8451	0.6146	0.4508	0.3436	0.2710	0.2200	0.1818	0.1538	0.1304
CNLM	0.9394	0.8889	0.8347	0.7787	0.7227	0.6673	0.6148	0.5647	0.5189
PNLM	0.9391	0.8967	0.8601	0.8263	0.7956	0.7638	0.7357	0.7088	0.6799
JSNLM	0.9391	0.8877	0.8355	0.7789	0.7256	0.6685	0.6217	0.5717	0.5215
ANLM	0.9373	0.8987	0.8683	0.8388	0.8044	0.7623	0.7083	0.6529	0.5910
SWNLM	0.9327	0.8899	0.8526	0.8193	0.7862	0.7548	0.7206	0.6908	0.6591

a measure of the structural similarity between the ground truth and the estimated images. Actually, SSIM test shows more consistency with the human visual system (HVS). We used BC as an alternative quality measure because of its relevance to the image contrast. We have shown the quantitative results for Cameraman, Lena, Boat and Fingerprint images in Tables 2 -13. The quantitative analysis based on PSNR is summarized in Table 2 to Table 5 where as mean SSIM values are listed in Table 6 to Table 9 and BC in Table 10 to Table 13, respectively. As one can see

TABLE 8. Comparison of experimental results on Boat image based on mean SSIM.

Method	mean SSIM								
	$\sigma = 5$	$\sigma = 10$	$\sigma = 15$	$\sigma = 20$	$\sigma = 25$	$\sigma = 30$	$\sigma = 35$	$\sigma = 40$	$\sigma = 45$
Noisy	0.8570	0.6484	0.4982	0.3959	0.3229	0.2696	0.2283	0.1955	0.1686
CNLM	0.9521	0.9018	0.8442	0.7868	0.7283	0.6751	0.6219	0.5726	0.5262
PNLM	0.9303	0.8702	0.8196	0.7766	0.7383	0.6997	0.6668	0.6368	0.6061
JSNLM	0.9517	0.9007	0.8462	0.7891	0.7358	0.6784	0.6278	0.5776	0.5359
ANLM	0.9289	0.8943	0.8557	0.8200	0.7837	0.7461	0.7032	0.6529	0.5988
SWNLM	0.9494	0.9070	0.8674	0.8307	0.7965	0.7624	0.7265	0.6943	0.5989

TABLE 9. Comparison of experimental results on Fingerprint image based on mean SSIM.

Method	mean SSIM								
	$\sigma = 5$	$\sigma = 10$	$\sigma = 15$	$\sigma = 20$	$\sigma = 25$	$\sigma = 30$	$\sigma = 35$	$\sigma = 40$	$\sigma = 45$
Noisy	0.9786	0.9232	0.8478	0.7697	0.6900	0.6173	0.5521	0.4940	0.4427
CNLM	0.9806	0.9623	0.9398	0.9139	0.8843	0.8510	0.8142	0.7765	0.7378
PNLM	0.9831	0.9616	0.9396	0.9116	0.8802	0.8439	0.8050	0.7689	0.7247
JSNLM	0.9823	0.9627	0.9422	0.9179	0.8895	0.8577	0.8252	0.7859	0.7520
ANLM	0.9794	0.9450	0.9130	0.8780	0.8402	0.8009	0.7650	0.7246	0.6881
SWNLM	0.9805	0.9592	0.9419	0.9227	0.9024	0.8802	0.8563	0.8310	0.8093

TABLE 10. Comparison of experimental results on Cameraman image based on BC.

Method	BC								
	$\sigma = 5$	$\sigma = 10$	$\sigma = 15$	$\sigma = 20$	$\sigma = 25$	$\sigma = 30$	$\sigma = 35$	$\sigma = 40$	$\sigma = 45$
Noisy	0.9844	0.9682	0.9555	0.9429	0.9303	0.9171	0.9048	0.8926	0.8817
CNLM	0.9975	0.9974	0.9953	0.9908	0.9856	0.9817	0.9782	0.9750	0.9715
PNLM	0.9948	0.9948	0.9949	0.9943	0.9933	0.9919	0.9907	0.9899	0.9884
JSNLM	0.9967	0.9970	0.9960	0.9919	0.9870	0.9817	0.9790	0.9753	0.9730
ANLM	0.9961	0.9959	0.9963	0.9955	0.9942	0.9927	0.9914	0.9892	0.9871
SWNLM	0.9974	0.9966	0.9972	0.9963	0.9952	0.9944	0.9921	0.9895	0.9868

TABLE 11. Comparison of experimental results on Lena image based on BC.

Method	BC								
	$\sigma = 5$	$\sigma = 10$	$\sigma = 15$	$\sigma = 20$	$\sigma = 25$	$\sigma = 30$	$\sigma = 35$	$\sigma = 40$	$\sigma = 45$
Noisy	0.9977	0.9897	0.9793	0.9698	0.9626	0.9564	0.9510	0.9453	0.9403
CNLM	0.9987	0.9982	0.9979	0.9981	0.9979	0.9975	0.9963	0.9958	0.9946
PNLM	0.9981	0.9966	0.9950	0.9943	0.9929	0.9931	0.9926	0.9927	0.9912
JSNLM	0.9986	0.9973	0.9972	0.9966	0.9968	0.9968	0.9958	0.9952	0.9940
ANLM	0.9985	0.9973	0.9966	0.9963	0.9958	0.9947	0.9944	0.9926	0.9912
SWNLM	0.9987	0.9983	0.9983	0.9981	0.9983	0.9982	0.9977	0.9975	0.9967

TABLE 12. Comparison of experimental results on Boat image based on BC.

Method	BC								
	$\sigma = 5$	$\sigma = 10$	$\sigma = 15$	$\sigma = 20$	$\sigma = 25$	$\sigma = 30$	$\sigma = 35$	$\sigma = 40$	$\sigma = 45$
Noisy	0.9936	0.9839	0.9710	0.9568	0.9420	0.9272	0.9131	0.9010	0.8916
CNLM	0.9964	0.9959	0.9948	0.9943	0.9937	0.9921	0.9918	0.9900	0.9879
PNLM	0.9948	0.9935	0.9922	0.9916	0.9912	0.9907	0.9900	0.9900	0.9909
JSNLM	0.9963	0.9955	0.9945	0.9942	0.9932	0.9925	0.9908	0.9894	0.9883
ANLM	0.9958	0.9957	0.9955	0.9950	0.9942	0.9937	0.9925	0.9918	0.9901
SWNLM	0.9962	0.9958	0.9961	0.9956	0.9951	0.9948	0.9939	0.9941	0.9917

from the above quantitative results, the proposed SWNLM outperforms the other NLM based techniques in most of the cases.

C. DISCUSSION

As discussed earlier, there are a variety of goodness-of-fit tests for checking normality. In this section, we first present

TABLE 13. Comparison of experimental results on Boat image based on BC.

Method	BC								
	$\sigma = 5$	$\sigma = 10$	$\sigma = 15$	$\sigma = 20$	$\sigma = 25$	$\sigma = 30$	$\sigma = 35$	$\sigma = 40$	$\sigma = 45$
Noisy	0.7344	0.7338	0.7322	0.7280	0.7254	0.7240	0.7202	0.7181	0.7158
CNLM	0.7349	0.7353	0.7334	0.7336	0.7328	0.7310	0.7306	0.7280	0.7285
PNLM	0.7350	0.7340	0.7333	0.7323	0.7322	0.7291	0.7260	0.7245	0.7196
JSNLM	0.7353	0.7334	0.7342	0.7321	0.7318	0.7313	0.7295	0.7282	0.7243
ANLM	0.7344	0.7356	0.7351	0.7351	0.7327	0.7322	0.7311	0.7301	0.7288
SWNLM	0.7356	0.7348	0.7346	0.7347	0.7342	0.7339	0.7329	0.7335	0.7347

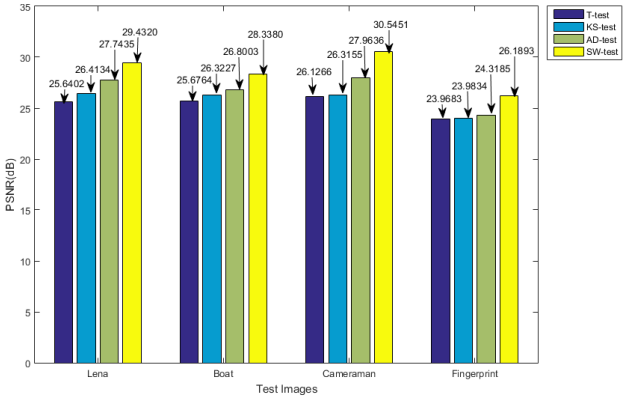

FIGURE 3. Denosing performance (based on PSNR) of NLM methodology with different statistical tests.

comparison among different statistical tests such as KS test, AD test, T-test, χ^2 test, JB test and SW test to facilitate sample selection for NLM estimation and, thereby, denoising the images. For this study, we compared the denoising performance of NLM filter with different statistical tests on noisy images of Lena, Boat, Cameraman and Fingerprint images corrupted with AWGN of noise standard deviation of 30 and plotted the result in terms of PSNR in a bar diagram (see Fig. 3). As expected, it shows that SW test is better than other statistical tests. This experiment was conducted with a similarity window of size 3×3 and a search window of size 21×21.

The disadvantage of the proposed SWNLM filter is its high time complexity compared to conventional NLM. The major reason behind this is the additional time taken for the SW test. In fact, a GPU implementation of the proposed filter (as in [46]) can substantially reduce its execution time. We carried out all our experiments with an Intel Core i7 CPU @3.40GHz processor and the proposed filter implemented on MATLAB 2018a (rev 9.4.0).

V. CONCLUSION

In this paper, a new NLM filter using Shapiro-Wilk statistical test have been presented. This study validates the use of SW statistic based similarity measure for sample selection to perform NLM estimation. In addition, we also considered the standard error in the computation to improve the results. Experiments were carried out on simulated images to validate the efficiency of the proposed method quantitatively as well as qualitatively. Assessments in terms of visual examinations and quality measures such as PSNR, mean SSIM, BC on simulated images with a range of noise levels shows the better performance of proposed framework compared to other NLM methods. Also, the proposed method achieves good noise reduction and detail preservation in different images.

REFERENCES

[1] P. Jain and V. Tyagi, "Spatial and frequency domain filters for restoration of noisy images," *IETE J. Educ.*, vol. 54, no. 2, pp. 108–116, 2013.

[2] I. T. Young and L. J. van Vliet, "Recursive implementation of the Gaussian filter," *Signal Process.*, vol. 44, no. 2, pp. 139–151, 1995.

[3] S. Haykin and B. Widrow, *Least-Mean-Square Adaptive Filters*, vol. 31. Hoboken, NJ, USA: Wiley, 2003.

[4] G. Z. Yang, P. Burger, D. N. Firmin, and S. R. Underwood, "Structure adaptive anisotropic image filtering," *Image Vis. Comput.*, vol. 14, no. 2, pp. 135–145, Mar. 1996.

[5] E. P. Simoncelli and E. H. Adelson, "Noise removal via Bayesian wavelet coring," in *Proc. Int. Conf. Image Process.*, vol. 1, Sep. 1996, pp. 379–382.

[6] J.-L. Starck, E. J. Candes, and D. L. Donoho, "The curvelet transform for image denoising," *IEEE Trans. Electron. Packag. Manuf.*, vol. 11, no. 6, pp. 670–684, Jun. 2002.

[7] H. Bhujle and S. Chaudhuri, "PCA based video denoising in a non-local means framework," in *Proc. 8th Indian Conf. Comput. Vis., Graph. Image Process.*, 2012, Art. no. 64.

[8] C. Tomasi and R. Manduchi, "Bilateral filtering for gray and color images," in *Proc. 6th Int. Conf. Comput. Vis.*, Jan. 1998, pp. 839–846.

[9] H. Takeda, S. Farsiu, and P. Milanfar, "Kernel regression for image processing and reconstruction," *IEEE Trans. Image Process.*, vol. 16, no. 2, pp. 349–366, Feb. 2007.

[10] K. Konstantinides, B. Natarajan, and G. S. Yovanof, "Noise estimation and filtering using block-based singular value decomposition," *IEEE Trans. Image Process.*, vol. 6, no. 3, pp. 479–483, Mar. 1997.

[11] T. Hong-Lei, "Non-local means denoising algorithm based on DCT," *Sci. Technol. Eng.*, vol. 11, p. 042, Nov. 2013.

[12] B. Cai, W. Liu, Z. Zheng, and Z. Wang, "A new similarity measure for non-local means denoising," in *Proc. CCF Chin. Conf. Comput. Vis.* Berlin, Germany: Springer, Sep. 2015, pp. 306–316.

[13] R. Verma and R. Pandey, "Non local means algorithm with adaptive isotropic search window size for image denoising," in *Proc. IEEE Annu. India Conf. (INDICON)*, Dec. 2015, pp. 1–5.

[14] C. Zuo *et al.*, "Rotation invariant similarity measure for non-local self-similarity based image denoising," in *Proc. IEEE Int. Conf. Image Process. (ICIP)*, Sep. 2015, pp. 1618–1622.

[15] H. Bhujle and S. Chaudhuri, "Novel speed-up strategies for non-local means denoising with patch and edge patch based dictionaries," *IEEE Trans. Image Process.*, vol. 23, no. 1, pp. 356–365, Jan. 2014.

[16] Y. Zhan, M. Ding, and X. Zhang, "Pixel-wise decay parameter adaption for nonlocal means image denoising," *J. Electron. Imag.*, vol. 22, no. 4, p. 043034, 2013.

[17] K. N. Chaudhury and A. Singer, "Non-local Euclidean medians," *IEEE Signal Process. Lett.*, vol. 19, no. 11, pp. 745–748, Nov. 2012.

[18] R. Yan, L. Shao, S. D. Cvetkovic, and J. Klijn, "Improved nonlocal means based on pre-classification and invariant block matching," *J. Display Technol.*, vol. 8, no. 4, pp. 212–218, Apr. 2012.

[19] C. A. Deledalle, V. Duval, and J. Salmon, "Non-local methods with shape-adaptive patches (NLM-SAP)," *J. Math. Imag. Vis.*, vol. 43, no. 2, pp. 103–120, Jun. 2012.
[20] S. Grewenig, S. Zimmer, and J. Weickert, "Rotationally invariant similarity measures for nonlocal image denoising," *J. Vis. Commun. Image Represent.*, vol. 22, no. 2, pp. 117–130, 2011.
[21] W. L. Zeng and X. B. Lu, "Region-based non-local means algorithm for noise removal," *Electron. Lett.*, vol. 47, no. 20, pp. 1125–1127, Sep. 2011.
[22] K. Zheng, W. Feng, and H. Chen, "An adaptive non-local means algorithm for image denoising via pixel region growing and merging," in *Proc. 3rd Int. Congr. Image Signal Process. (CISP)*, vol. 2, Oct. 2010, pp. 621–625.
[23] V. Duval, J.-F. Aujol, and Y. Gousseau, "On the parameter choice for the non-local means," *SIAM J. Imag. Sci.*, p. 37, 2010.
[24] R. Vignesh, B. T. Oh, and C. C. J. Kuo, "Fast non-local means (NLM) computation with probabilistic early termination," *IEEE Signal Process. Lett.*, vol. 17, no. 3, pp. 277–280, Mar. 2010.
[25] Z. Ji, Q. Chen, Q.-S. Sun, and D.-S. Xia, "A moment-based nonlocal-means algorithm for image denoising," *Inf. Process. Lett.*, vol. 109, nos. 23–24, pp. 1238–1244, 2009.
[26] Y. Lou, P. Favaro, S. Soatto, and A. Bertozzi, "Nonlocal similarity image filtering," in *Proc. Int. Conf. Image Anal. Process.* Berlin, Germany: Springer, Sep. 2009, pp. 62–71.
[27] S. Zimmer, S. Didas, and J. Weickert, "A rotationally invariant block matching strategy improving image denoising with non-local means," in *Proc. Int. Workshop Local Non-Local Approximation Image Process.*, 2008, pp. 135–142.
[28] Y. Liu, J. Wang, X. Chen, Y. Guo, and Q. Peng, "A robust and fast non-local means algorithm for image denoising," *J. Comput. Sci. Technol.*, vol. 23, no. 2, pp. 270–279, Apr. 2008.
[29] T. Brox and D. Cremers, "Iterated nonlocal means for texture restoration," in *Proc. Int. Conf. Scale Space Variational Methods Comput. Vis.* Berlin, Germany: Springer, May 2007, pp. 13–24.
[30] A. Buades, B. Coll, and J.-M. Morel, "A review of image denoising algorithms, with a new one," *Multiscale Model. Simul.*, vol. 4, no. 2, pp. 490–530, 2005.
[31] A. Buades, B. Coll, and J.-M. Morel, "A non-local algorithm for image denoising," in *Proc. IEEE Comput. Soc. Conf. Comput. Vis. Pattern Recognit.*, San Diego, CA, USA, vol. 2, Jun. 2005, pp. 60–65.
[32] J. V. Manjón, J. Carbonell-Caballero, J. J. Lull, G. García-Martí, L. Martí-Bonmatí, and M. Robles, "MRI denoising using non-local means," *Med. Image Anal.*, vol. 12, no. 4, pp. 514–523, 2008.
[33] S. Aja-Fernandez, C. Alberola-López, and C.-F. Westin, "Noise and signal estimation in magnitude MRI and rician distributed images: A LMMSE approach," *IEEE Trans. Image Process.*, vol. 17, no. 8, pp. 1383–1398, Aug. 2008.
[34] P. Coupè, P. Yger, S. Prima, P. Hellier, C. Kervrann, and C. Barillot, "An optimized blockwise nonlocal means denoising filter for 3-D magnetic resonance images," *IEEE Trans. Med. Imag.*, vol. 27, no. 4, pp. 425–441, Apr. 2008.
[35] F. J. Massey, Jr., "The Kolmogorov-Smirnov test for goodness of fit," *J. Amer. Statist. Assoc.*, vol. 46, no. 253, pp. 68–78, 1951.
[36] C. M. Jarque and A. K. Bera, "A test for normality of observations and regression residuals," *Int. Stat. Rev./Revue Internationale Statistique*, vol. 55, no. 2, pp. 163–172, 1987.
[37] S. S. Shapiro and M. B. Wilk, "An analysis of variance test for normality (complete samples)," *Biometrika*, vol. 52, nos. 3–4, pp. 591–611, 1965.
[38] P. Royston, "Remark AS R94: A remark on algorithm AS 181: The W-test for normality," *J. Roy. Stat. Soc. C (Appl. Statist.)*, vol. 44, no. 4, pp. 547–551, 1995.
[39] *Normal Difference Distribution*. Accessed: Apr. 26, 2018. [Online]. Available: http://mathworld.wolfram.com/NormalDifference-Distribution.html
[40] M. Kurtz, *Handbook of Applied Mathematics for Engineers and Scientists*. London, U.K.: Chapman and Hall, 1991.
[41] *Denoising Results*. Accessed: May 2018. [Online]. Available: http://people.kyb.tuebingen.mpg.de/pgehler/poedges/code.html
[42] Y. Wu, B. Tracey, P. Natarajan, and J. P. Noonan, "James–stein type center pixel weights for non-local means image denoising," *IEEE Signal Process. Lett.*, vol. 20, no. 4, pp. 411–414, Apr. 2013.
[43] Y. Fisher, *Pixelized Data*. London, U.K.: Springer-Verlag, 1995.
[44] Z. Wang, A. C. Bovik, H. R. Sheikh, and E. P. Simoncelli, "Image quality assessment: From error visibility to structural similarity," *IEEE Trans. Image Process.*, vol. 13, no. 4, pp. 600–612, Apr. 2004.
[45] A. Bhattacharyya, "On a measure of divergence between two multinomial populations," *Sankhyā Indian J. Stat.*, vol. 7, no. 4, pp. 401–406, Jul. 1946. [Online]. Available: https://www.jstor.org/stable/25047882
[46] A. H. K. Upadhya, B. Talawar, and J. Rajan, "GPU implementation of non-local maximum likelihood estimation method for denoising magnetic resonance images," *J. Real-Time Image Process.*, vol. 13, no. 1, pp. 181–192, 2017.

W. YAMANAPPA received the B.E. degree in computer science and engineering from SJCE Mysore and the M.Tech. degree in computer science and engineering from the National Institute of Technology Karnataka, Mangalore, where he is currently pursuing the Ph.D. degree in computer science. His areas of research are image processing and medical image enhancement.

P. V. SUDEEP received the B.Tech. and M.Tech. degrees from the University of Kerala, India, and the Ph.D. degree from the National Institute of Technology, Tiruchirappalli, India. He is currently an Assistant Professor with the Department of Electronics and Communication Engineering, National Institute of Technology Calicut, Kerala. His area of interest includes medical image analysis and machine learning.

M. K. SABU received the M.C.A. degree from the Government Engineering College, Thrissur, Kerala, and the Ph.D. degree in computer science from the School of Computer Sciences, MG University, Kottayam, Kerala. He is currently an Associate Professor with the Department of Computer Applications, Cochin University of Science and Technology, Kochi, India. His areas of interest are optimization techniques and data mining.

JENY RAJAN received the M.Tech. degree from the University of Kerala, India, and the Ph.D. degree from the University of Antwerp, Belgium. He is currently an Assistant Professor with the Department of Computer Science and Engineering, National Institute of Technology Karnataka. His main research interests are MRI, OCT, and ultrasound image processing.